Journal of Power Sources 240 (2013) 184–192

Contents lists available at SciVerse ScienceDirect

Journal of Power Sources

journal homepage: www.elsevier.com/locate/jpowsour

Online battery state of health estimation based on Genetic Algorithm for electric and hybrid vehicle applications☆

Zheng Chen, Chunting Chris Mi*, Yuhong Fu, Jun Xu, Xianzhi Gong

Department of Electrical and Computer Engineering Department, University of Michigan-Dearborn, 4901 Evergreen Road, Dearborn, MI 48188, USA

HIGHLIGHTS

- Proposed an online battery state of health estimation method based on battery model parameters.
- Genetic Algorithm is employed to estimate the battery parameters.
- Determine the battery SOH in real time based on estimated battery parameters.
- Developed a formula to calculate the SOH based on the estimated diffusion capacitance.
- Temperature influence is considered to improve the robustness of SOH estimation.

ARTICLE INFO

Article history:
Received 21 January 2013
Received in revised form
26 March 2013
Accepted 27 March 2013
Available online 11 April 2013

Keywords:
State of health (SOH)
Electric vehicles
Battery model
Genetic algorithm
Diffusion capacitance
Prediction-error minimization

ABSTRACT

State of health (SOH) of batteries in electric and hybrid vehicles can be observed using some battery parameters. Based on a resistance–capacitance circuit model of the battery and data obtained from abundant experiments, it was observed that the diffusion capacitance shows great correlation with SOH of a lithium-ion battery. However, accurate measurement of this diffusion capacitance in real time in an electric or hybrid electric vehicle is not practical. In this paper, Genetic Algorithm (GA) is employed to estimate the battery model parameters including the diffusion capacitance in real time using measurement of current and voltage of the battery. The battery SOH can then be determined using the identified diffusion capacitance. Temperature influence is also considered to improve the robustness and precision of SOH estimation results. Experimental results on various batteries further verified the proposed method.

1. Introduction

Lithium-ion batteries are considered the only viable solution for electric drive vehicles (EDVs), including hybrid electric vehicles (HEVs), plug-in HEVs (PHEVs) and battery electric vehicles (BEVs). Battery safety and reliability are critical for the large-scale penetration of EDVs in the market place. A battery management system (BMS) is essential to manage, observe and protect the battery for safe and reliable operations of the vehicle. State of charge (SOC) and state of health (SOH) are very basic functions of the BMS [1–6].

Battery SOC is the ratio of available capacity and nominal capacity. It can be calculated through coulomb counting method, which is simple, direct and reliable [7]. However, this method relies on the knowledge of initial SOC. Other intelligent methods, such as neural network and extended Kalman filter (EKF), have been introduced to enhance the accuracy and precision of SOC calculations by removing measurement error and noise, as well as reliance on initial SOC [5].

Battery SOH describes the battery performance at the present time compared with the performance at ideal conditions and when the battery was new [5,8–16]. It is a measurement that reflects the battery performance and health status. Research on battery SOH has attracted wide attentions due to its importance in EDVs. In theory, by measuring the battery capacity through charging and discharging with the referenced method at certain temperature, the present capacity, hence the SOH, can be obtained.

Typically, there exist several methods to derive a battery SOH, such as comparing the internal resistance [5,11], total available capacity [7], voltage drop [17], self-discharge, number of cycles, etc. Jonghoon Kim and Cho [5] proposed a method based on an EKF

☆ This project is supported by the US DOE under grant DE-EE0002720.
* Corresponding author. Tel.: +1 313 583 6434.
E-mail address: chrismi@umich.edu (C.C. Mi).

0378-7753/$ – see front matter © 2013 Elsevier B.V. All rights reserved.
http://dx.doi.org/10.1016/j.jpowsour.2013.03.158

combined with a per-unit system to identify suitable battery model parameters, which can be utilized to estimate SOC and SOH for a lithium-ion battery. The main work of Ref. [5] was to estimate SOC based on EKF and an accurate battery model. In addition, the diffusion resistance in the model proposed in the paper was changeable with battery age. It needed some particular charge/discharge steps to estimate the battery diffusion resistance, which increases the complexity of estimating the SOH. Besides, it did not consider temperature influence. In Ref. [7], the battery SOH can be determined by fully charged and discharged capacity. It was time consuming, temperature-dependent, and usually hard to realize after equipped in a vehicle. C. R. Gould et al. [15] described a new battery model and determined the SOH through subspace parameter estimation and state-observer techniques. It mainly focused on a novel battery model and a predictor/corrector observer. Based on the observer to adaptively estimate and converge on battery functionality indicators, the SOH can be estimated accordingly. They focused on a lead acid battery, whose characteristic is different from lithium-ion battery, and developed a linear equation between battery SOH and capacitance. It only considered 20% capacity drop which was too narrow to estimate the battery SOH precisely.

Some researchers have proposed other methods to estimate the SOH through analyzing the battery internal parameters. Reference [12] presented a complementary cooperation algorithm based on dual EKF combined with pattern recognition as an application of Hamming neural network to identify suitable battery model parameters for improved SOC/capacity estimation and SOH prediction. It needed about 6000 s to acquire the data to identify the battery parameters. Therefore it needed larger storage for data, and to wait longer time to estimate the SOH. A method to identify the internal resistance in a hybrid vehicles was presented and a special purpose model derived from an equivalent circuit was developed in Ref. [11]. This model contained parameters depending on the degradation of the battery cell. This method needed specific signal intervals occurring during normal operation of the battery in a hybrid vehicle which limits its application.

Battery SOH is defined as:

$$h = \frac{C_{bat}}{C_{nominal}} \times 100\% \tag{1}$$

where h is SOH, C_{bat} is the present capacity and $C_{nominal}$ is the nominal capacity of the battery.

While using the above equation for SOH calculations, some difficulties arise:

- The battery needs to be fully charged and discharged to determine its present capacity, which is not realistic especially when the battery is already installed in an EDV;
- The battery capacity will change with temperature and with different charge/discharge current profiles.

In this paper, an online SOH identification method is proposed through estimating the battery diffusion capacitance of a two-order resistance–capacitance model instead of direct measurement of battery capacity. From experiments of the battery, we have found direct linkage between the battery's diffusion capacitance and the total available capacity. However, in order to estimate SOH using the diffusion capacitance, we must estimate the voltage drop on the capacitance. If the battery is under rest for a very long period of time, such as 3 h, we can assume the initial voltage drop on the capacitance is zero. When the vehicle is running, it is difficult to obtain voltage drop on the capacitance. To overcome this problem, we introduce the genetic algorithm (GA) to estimate the voltage drop on the capacitance and the battery open circuit voltage in the battery model through the use of measured battery current and terminal voltage. The diffusion capacitance, hence, the SOH is then determined.

GA is an effective tool to estimate the model parameters of a nonlinear system. Genetic algorithm is inspired by natural selection and biological evolution, and is an efficient method for solving both constrained and unconstrained optimization problems through repeatedly modifying a population of individual solutions. GA can be found with wide applications in bioinformatics, computational science, engineering, mathematics, physics, and other related fields [18–22]. Typically, GA requires:

- A genetic representation of the solution, which is so-called the population;
- A fitness function which is utilized to evaluate the solution.

A typical representation of the population is bit strings. Other representations may also be introduced, like double vector. All the populations can be used in the same way, which makes genetic algorithms more convenient to realize crossover, mutation and elite selection. A fitness function is defined to show the performance for each population. Once the genetic representation and the fitness function are defined, GA proceeds to initialize a population of solutions (usually randomly) and then to improve it through repetitive application of the mutation, crossover, inversion and selection operators.

At each step, the GA selects individuals at random from the current population to be parents and uses them to produce the children for the next generation. Over successive generations, the population evolves towards an optimal solution. GA has been successfully applied in the multi objective optimization of HEV fuel economy and emissions using the self-adaptive differential evolution algorithm [22]. In this paper, GA is proposed to estimate the battery parameters based on prediction-error minimization method.

The rest of the paper is arranged as follows. Section 2 introduces the battery model that is used for SOH estimation. Section 3 explains GA and the parameter identification method. Section 4 analyzes the uniqueness of the model and convergence of the proposed GA algorithm. The experiment verification is presented in Section 5. We also add the temperature influence and build an observer of SOH with ambient temperature from 0 °C to 40 °C. Some conclusion and next step work are finally given in Section 6.

2. Proposed method

An equivalent circuit model with one open circuit voltage source, two parallel resistor–capacitor networks and a series resistor, as shown in Fig. 1, is introduced to simulate the battery dynamic and static performance [2,3,5,12,23–25]. The open circuit voltage source, which is parameterized as a nonlinear function of battery SOC and the open circuit voltage, is to describe the open circuit

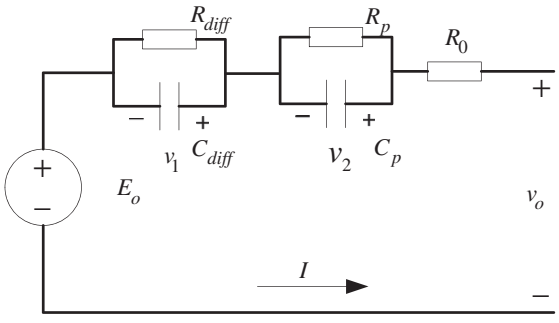

Fig. 1. Equivalent circuit model of battery cell.

voltage characteristic at different SOC. The two parallel resistor–capacitor networks represent the time-dependent polarization and diffusion effects of the cell. The series resistor is to describe the immediate voltage drop after an excitation current in the battery. The parameters change gradually as the battery ages. The proposed method is to identify the parameters online and determine the SOH according to the identified parameters. This way we can obtain the SOH in real time. In order to get accurate model parameters, a particular length of data including battery current and terminal voltage, as well as battery surface temperature is needed. Through experiment, we have found that, in a short period of time, e.g. less than 30 s, if the battery charges/discharges within 2 C rate, the open circuit voltage can be regarded as unchanged, where C denotes the battery rated capacity in ampere-hours.[1] We also assume that the battery parameters, including the diffusion capacitance, diffusion resistance, etc., will remain unchanged during this time interval. During vehicle operation, or when the vehicle is charged, or right after the vehicle is turned off, we can select a time window of 30 s to measure the battery voltage, current, and temperature so as to use the GA algorithm to estimate the battery model parameters, as long as the discharge/charge rate is less than 2 C.

In this proposed method, we use GA to estimate the open circuit voltage E_o and voltage drops on C_{diff} and C_p from measured battery terminal voltage, current, and temperature within the 30 s interval. Based on these estimated voltages, we use iterative prediction-error minimization algorithm (which will be discussed in the next section) to estimate the battery parameters. Through the recursive iteration and convergence ability of GA, the voltages can be found and as such, the battery model can be identified accordingly. We then use the identified diffusion capacitance to calculate the battery SOH.

3. Genetic algorithm and parameter identification

3.1. Parameter identification

From Fig. 1, the following equations can be obtained:

$$v_o = E_o + v_1 + v_2 + iR_0 \tag{2}$$

$$i = \frac{v_1}{R_{diff}} + C_{diff}\frac{dv_1}{dt} = \frac{v_2}{R_p} + C_p\frac{dv_2}{dt} \tag{3}$$

where v_o is the battery terminal voltage, i is the battery current, R_0, R_{diff}, C_{diff}, R_p and C_p are battery parameters which reflect the battery dynamic response and capacity. v_1 is the voltage drop on capacitor C_{diff}, v_2 the voltage drop on capacitor C_p, and E_o is the battery internal open circuit voltage.

For further analysis, we choose the voltage drop on the capacitors as the state variables. The state space equation can then be expressed as:

$$\dot{x} = \begin{bmatrix} -\frac{1}{R_{diff}C_{diff}} & 0 \\ 0 & -\frac{1}{R_pC_p} \end{bmatrix}\cdot x + \begin{bmatrix} \frac{1}{C_{diff}} \\ \frac{1}{C_p} \end{bmatrix}\cdot i \tag{4}$$

$$y = [1 \quad 1]\cdot x + E_o + i\cdot R_0 \tag{5}$$

where $x = [v_1 \quad v_2]^T$, $[]^T$ denotes the transposition of a matrix, y is the estimated battery terminal voltage.

[1] The capacity (or SOC) change is less than 1.7% (2 C * 30 s/3600 s = 1.7%).

Define $A = \begin{bmatrix} -1/\left(R_{diff}C_{diff}\right) & 0 \\ 0 & -1/(R_pC_p) \end{bmatrix}$, $B = \begin{bmatrix} 1/C_{diff} \\ 1/C_p \end{bmatrix}$, $C = [1\ 1]$, $D = R_0$, $u = i$, then Eqs. (4) and (5) can be written as a standard form:

$$\begin{cases} \dot{x}(t) = Ax(t) + Bu \\ y(t) = Cx(t) + Du + E_o \end{cases} \tag{6}$$

Based on Eq. (6), we can get the system output:

$$y(t) = e^{p_1 t}v_1(0) + \int_0^t e^{p_1(t-\tau)}q_1u(\tau)d\tau + e^{p_2 t}v_2(0) + \int_0^t e^{p_2(t-\tau)}q_2u(\tau)d\tau + E_o + iR_0 \tag{7}$$

where $p_1 = -1/(R_{diff}C_{diff})$, $p_2 = -1/(R_pC_p)$, $q_1 = 1/C_{diff}$, $q_2 = 1/C_p$, u is the input-battery current, $v_1(0)$, and $v_2(0)$ are the initial voltage drop on of C_{diff} and C_p. We can find that the system output, i.e. battery voltage, has a strong relationship with $v_1(0)$, $v_2(0)$, and E_o. As E_o changes with time, we can only use a short time period to estimate the system parameters, so some recursive methods which can estimate the system parameters, like Kalman filter, cannot be applied as it needs the recursive computation to make the system parameters converged.

Iterative prediction-error minimization (PEM) method, as a general estimation method, is selected to estimate the model parameters. PEM uses optimization to minimize the cost function, defined as follows for scalar outputs.

$$V_n = \sum_{t=1}^{N} e^2(t) \tag{8}$$

where $e(t)$ is the difference between the measured output and the predicted output of the model, and in this paper, $e(t) = y - v_o$. We use least-square algorithm to realize PEM for minimizing the cost function. The fitness function is to compare the model output (y) and measured output (v_o), and is based on the following equation.

$$\text{Fitness} = \left(1 - \frac{\sqrt{V_n}}{\sqrt{\sum(v_o - \bar{v}_o)^2}}\right) \times 100\% \tag{9}$$

where $\bar{v}_o$ is the average value of v_o over the time period the parameters are estimated. If y is equal to v_o, then the fitness value equals 100%, which is also the maximum value of fitness.

Transfer (6) into the discrete form:

$$\begin{cases} x(kT + T) = A_dx(kT) + B_du(kT) \\ y(kT) = C_dx(kT) + D_du(kT) + E_o \end{cases} \tag{10}$$

where T is the sample time interval, k is the time step, and $A_d = e^{AT}$, $B_d = \int_0^T e^{A\tau}Bd\tau$, $C_d = C$, $D_d = D$. We can get:

$$A_d = \begin{bmatrix} a_{11} & 0 \\ 0 & a_{22} \end{bmatrix} = \begin{bmatrix} e^{-\frac{T}{R_{diff}C_{diff}}} & 0 \\ 0 & e^{-\frac{T}{R_pC_p}} \end{bmatrix},$$

$$B_d = \begin{bmatrix} b_{d1} \\ b_{d2} \end{bmatrix} = \begin{bmatrix} \frac{1}{C_{diff}}\int_0^T e^{-\frac{\tau}{R_{diff}C_{diff}}}d\tau \\ \frac{1}{C_p}\int_0^T e^{-\frac{\tau}{R_pC_p}}d\tau \end{bmatrix} = \begin{bmatrix} R_{diff}\left(1 - e^{-\frac{T}{R_{diff}C_{diff}}}\right) \\ R_p\left(1 - e^{-\frac{T}{R_pC_p}}\right) \end{bmatrix}.$$

Here we assume the initial state $X(0) = [v_1(0) \quad v_2(0)]^T$ In order to estimate the parameters in Eq. (10), the z-transform is applied:

$$X[z] = (zI - A_d)^{-1}[zX(0) + B_d U[z]] \tag{11}$$

$$\begin{aligned} Y[z] &= C_d \cdot X[z] + D_d \cdot U[z] + E_o \\ &= C_d \cdot (zI - A_d)^{-1}[zX(0) + B_d U[z]] + D_d \cdot U[z] + E_o \\ &= \frac{zv_1(0) + b_{d1}U[z]}{z - a_{11}} + \frac{zv_2(0) + b_{d2}U[z]}{z - a_{22}} + D_d U[z] + E_o \end{aligned} \tag{12}$$

where $X[z]$, $Y[z]$, and $U[z]$ are the z-transform of $x(kT)$, $y(kT)$ and $u(kT)$.

Define $Y_d(z) = Y[z] - E_o$ and Eq. (12) can be transferred into:

$$\begin{aligned} &z^2 Y_d[Z] - zy_d(1) - z^2 y_d(0) - (a_{11} + a_{22})zY_d[Z] + (a_{11} + a_{22})zy_d(0) + a_{11}a_{22}Y_d[Z] \\ &= D_d z^2 U[z] + (b_{d2} + b_{d1} - a_{11}D_d - a_{22}D_d)zU[z] + (D_d a_{11}a_{22} - a_{22}b_{d1} - a_{11}b_{d2})U[z] + (z - a_{22})zv_1(0) + (z - a_{11})zv_2(0) - zy_d(1) \\ &\quad - z^2 y_d(0) + (a_{11} + a_{22})zy_d(0) \\ &= D_d z^2 U[z] + (b_{d2} + b_{d1} - a_{11}D_d - a_{22}D_d)zU[z] + (D_d a_{11}a_{22} - a_{22}b_{d1} - a_{11}b_{d2})U[z] + z^2[v_1(0) + v_2(0) - y_d(0)] \\ &\quad - z[a_{22}v_1(0) + a_{11}v_2(0) + y_d(1)] + (a_{11} + a_{22})zy_d(0) \\ &= D_d z^2 U[z] + (b_{d2} + b_{d1} - a_{11}D_d - a_{22}D_d)zU[z] - z^2 D_d u(0) + (D_d a_{11}a_{22} - a_{22}b_{d1} - a_{11}b_{d2})U[z] - z[a_{22}v_1(0) + a_{11}v_2(0) + y_d(1)] \\ &\quad + (a_{11} + a_{22})zy_d(0) \\ &= D_d z^2 U[z] + (b_{d2} + b_{d1} - a_{11}D_d - a_{22}D_d)zU[z] - z^2 D_d u(0) + (D_d a_{11}a_{22} - a_{22}b_{d1} - a_{11}b_{d2})U[z] - (b_{d2} + b_{d1} - a_{11}D_d - a_{22}D_d)zu(0) \\ &\quad + (b_{d2} + b_{d1} - a_{11}D_d - a_{22}D_d)zu(0) - z[a_{22}v_1(0) + a_{11}v_2(0) + a_{11}v_1(0) + a_{22}v_2(0) + b_{d1}u(0) + b_{d2}u(0) + D_d u(1)] \\ &\quad + (a_{11} + a_{22})zy_d(0) \\ &= D_d z^2 U[z] + (b_{d2} + b_{d1} - a_{11}D_d - a_{22}D_d)zU[z] - z^2 D_d u(0) + (D_d a_{11}a_{22} - a_{22}b_{d1} - a_{11}b_{d2})U[z] - (b_{d2} + b_{d1} - a_{11}D_d - a_{22}D_d)zu(0) \\ &\quad + (-a_{11}D_d - a_{22}D_d)zu(0) - z[a_{22}v_1(0) + a_{11}v_2(0) + a_{11}v_1(0) + a_{22}v_2(0) + D_d u(1)] + (a_{11} + a_{22})z[v_1(0) + v_2(0) + D_d u(0)] \\ &= D_d z^2 U[z] - zD_d u(1) - z^2 D_d u(0) + (b_{d2} + b_{d1} - a_{11}D_d - a_{22}D_d)zU[z] - (b_{d2} + b_{d1} - a_{11}D_d - a_{22}D_d)zu(0) \\ &\quad + (D_d a_{11}a_{22} - a_{22}b_{d1} - a_{11}b_{d2})U[z] \end{aligned} \tag{13}$$

where $y_d(0)$, and $y_d(1)$ are the battery voltage at $t = 0$, and $t = T$. $u(0)$, and $u(1)$ are the battery current at $t = 0$, and $t = T$ respectively.

So Eq. (13) can be transferred into differential equation:

$$\begin{aligned} &Y_d[kT + 2T] - (a_{11} + a_{22})Y_d[kT + T] + a_{11}a_{22}Y_d[kT] \\ &= D_d u[kT + 2T] + [b_{d2} + b_{d1} - a_{11}D_d - a_{22}D_d]u[kT + T] \\ &\quad + [D_d a_{11}a_{22} - a_{22}b_{d1} - a_{11}b_{d2}]u[kT] \end{aligned} \tag{14}$$

Suppose we have n sets of data and define:

$$P_d = [a_{11} + a_{22} \quad -a_{11}a_{22} \quad D_d \quad b_{d2} + b_{d1} - a_{11}D_d - a_{22}D_d \quad D_d a_{11}a_{22} - a_{22}b_{d1} - a_{11}b_{d2}]^T$$

$$Y_d = [Y_d(kT + 2T) \quad Y_d(kT + 3T) \quad \dots \quad Y_d(kT + nT + T)]^T$$

Then Eq. (14) can be changed into:

$$H_d = \begin{bmatrix} Y_d(kT + T) & Y_d(kT) & U(kT + 2T) & U(kT + T) & U(kT) \\ Y_d(kT + 2T) & Y_d(kT + T) & U(kT + 3T) & U(kT + 2T) & U(kT + T) \\ \vdots & \vdots & \vdots & \vdots & \vdots \\ Y_d(kT + nT) & Y_d(kT + nT - T) & U(kT + nT + T) & U(kT + nT) & U(kT + nT - T) \end{bmatrix}$$

$$Y_d = H_d \cdot P_d \tag{15}$$

The least-square algorithm can be applied to estimate the model parameters based on the following calculation.

$$P_d = \left(H_d^T \cdot H_d\right)^{-1} \cdot H_d^T \cdot Y_d \tag{16}$$

where $()^{-1}$ denotes the inverse of a matrix. As such, the battery parameters can be obtained based on the estimated P_d accordingly. So we need to determine E_o in advance to calculate Y_d and estimate the battery parameters. In order to calculate the fitness value in Eq. (9), we need to calculate the model output based on Eqs. (7) and (10), we need to know $v_1(0)$ and $v_2(0)$ ahead, which can be within the constraint of difference between battery terminal voltage $y(kT)$ and the open circuit voltage E_o. GA supplies an efficient way to estimate these values based on the fitness function.

3.2. Genetic algorithm

Typically, GA consists of encoding, selection, mutation and crossover [18–22]. The most used way of encoding is a binary string. During each successive generation, some of the existing population is selected to generate the next offspring and this process is the so-called selection. A proportion of the existing population is regarded as the elitists and selected as the next offspring directly without any change. The criterion of the selection is based on the fitness function and the constraint. The crossover process is to hybridize the chromosome of the parent and generate the next offspring and the mutation process's function is to mutate some bits in the chromosome randomly or uniformly. The main purpose

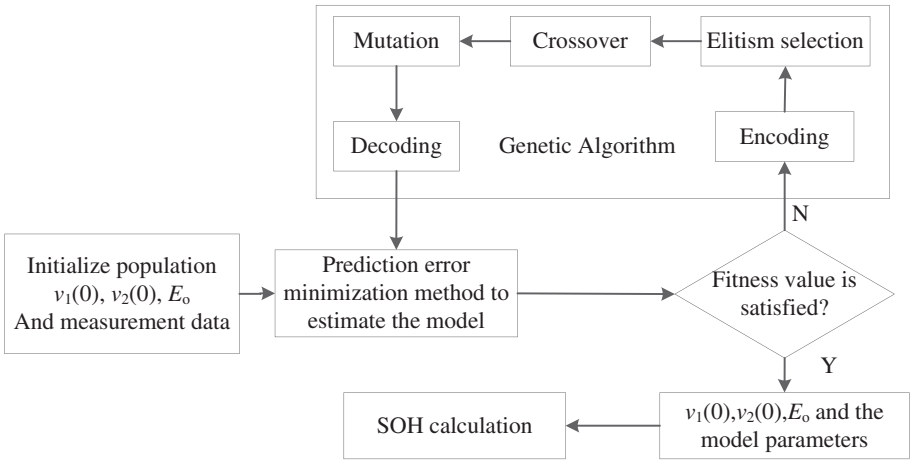

Fig. 2. The parameter identification using GA.

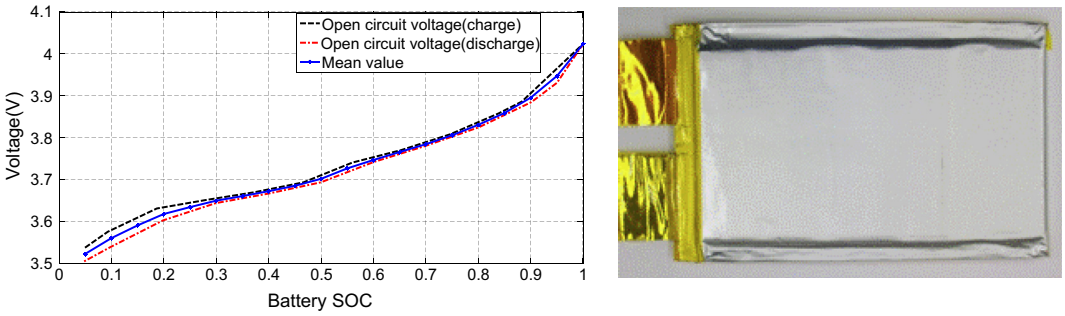

Fig. 3. The battery open circuit voltage versus SOC. (a) Open circuit voltage versus SOC; (b) Pouch cell battery.

of mutation is to prevent falling all solutions in population into a local optimum of solved problem. Finally, the above processes result in the next generation population of chromosomes which is different from the previous one. Generally the average fitness value will increase after processes. Although crossover and mutation are known as the main genetic operators, it is possible to use other operators such as regrouping, colonization–extinction, or migration in genetic algorithms. This generational process is repeated until a termination condition has been reached. Common terminating conditions are: (1). A solution is found that satisfies the minimum criteria; (2). Allocated budget, like time or generations reached. (3). The setting fitness value has been found.

Based on the above analysis, the SOH realization is shown in Fig. 2, which combines the battery model parameter identification along with GA. The process is realized in Matlab/Simulink.[2] The calculation process is repetitive according to the fitness value. If the fitness value is not satisfied, GA will take a series of actions, including elitism selection, crossover and mutation based on the fitness value of each individual, and output the new individuals, i.e. $v_1(0)$, $v_2(0)$, and E_o for the next cyclic calculation. The repetition continues and terminates until the fitness value is larger than the boundary value and the current parameters will be regarded as the identified system parameters. Based on the identified diffusion capacitance and the built relationship between diffusion capacitance and battery SOH, the battery SOH can be estimated. From Eq. (9), the maximum value of the fitness function is 100%. Due to the existence of noise of the measured current and terminal voltage, it is impossible to fit the curve with fitness value of 100%. In this paper, if the fitness of the model output reaches 95%, the model can be considered to simulate the system's performance, and the GA algorithm terminates.

4. Convergence analysis

In order to prove the convergence of the proposed GA for battery parameter estimation, we need to prove that:

- There is a unique solution of the battery model;
- The proposed algorithm converges.

In Eq. (6), as $C = [1\ 1]$ is definite, according to the proof in Ref. [26] (pp. 161–167), we concluded that there is a unique solution for the system parameters.

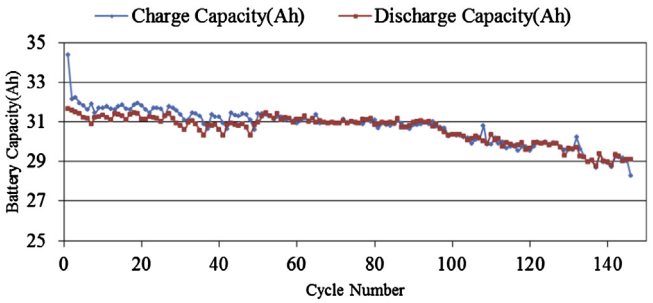

Fig. 4. Battery capacity variation versus charge/discharge cycle.

[2] Matlab is a high-level language for numerical computation, and programming. It is easy to use it to analyze data, develop algorithms, and build the models. Simulink, which is integrated with Matlab, provides a user-friendly interface, customizable block libraries, strong solvers for simulating dynamic systems, and fast auto-code generation for embedded systems.

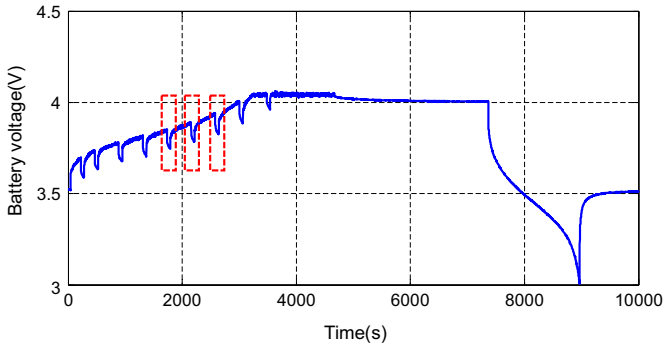

Fig. 5. Measured battery terminal voltage in the 102nd cycle.

The convergence rate of genetic algorithms is addressed using Markov chain analysis [20,21,27]. We can describe an elitist GA using mutation, recombination and selection as a discrete stochastic process. Evaluating the eigenvalues of the transition matrix of the Markov chain we can prove that the convergence rate of a GA is determined by the second largest eigenvalue of the transition matrix.

G. Rudolph [20] analyzed the convergence properties of the canonical genetic algorithm with crossover, mutation and selection by means of homogeneous finite Markov chain analysis, which showed that the canonical GA will never converge to the global optimum as a result of unceasing selection, crossover and mutation. However, he also proved that the canonical GA which can maintain the best solution found over time after selection converged to the global optimum. Besides, the canonical GA can reach any state infinite times with probability one regardless of the initial states. Theoretically, this means the premature convergence cannot occur provided that the mutation probability is larger than zero. Practically this means even if premature convergence can occur, it will not persist indefinitely. Therefore, GA with an arbitrary initial population converges to the global optimum if the following assumptions are fulfilled [20,27]:

- Selection chooses the elitist individual from parents and offspring.
- Each state is reachable from any other state.

Based on the above theorems, GA can reach any state. If the best individual can be selected, the convergence to the optimum value can be assured, thus the algorithm can converge to the optimal point without considering the initial input. During the process of GA operation to find the optimal value, the mutation coefficient, the population and the elitism of the population for GA is set to 0.05, 12 and 2 respectively. Therefore the convergence of the proposed method can be assured.

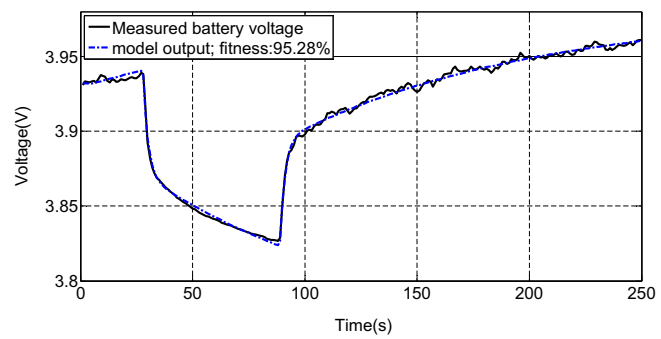

Fig. 6. Comparison of identified and measured battery terminal voltage.

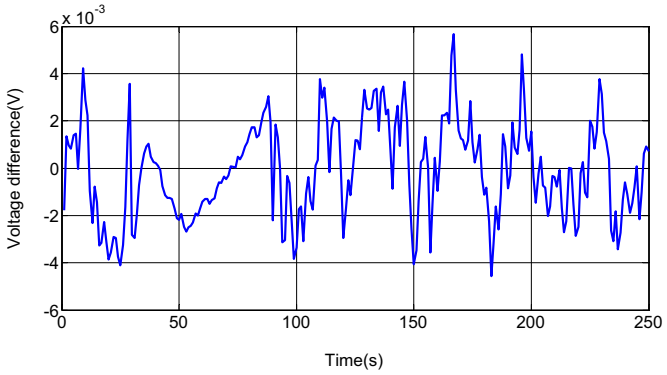

Fig. 7. Differences between measured and estimated battery terminal voltage.

5. Experiment validation

A pouch cell lithium-ion battery is tested repeatedly as well as at different ambient temperatures. The battery has a rated capacity of 32 Ah, fully charged voltage of 4.05 V, and cut-off voltage of 3 V. The open circuit voltage E_o and the battery cell are shown in Fig. 3, which ranges from 3.5 V to 4.05 V.

In order to realize online parameter estimation based on GA, some constraints should be considered which includes the restriction of $v_1(0)$ and $v_2(0)$, and the open circuit voltage E_o.

$$\begin{cases} v_1(0)+v_2(0)+E_o \le v_o \quad (\text{if } u(0)\ge 0) \\ v_1(0)+v_2(0)+E_o > v_o \quad (\text{if } u(0)<0) \\ -0.5 < v_1(0) < 0.5 \\ -0.5 < v_2(0) < 0.5 \\ 3.5 < E_o < 4.05 \\ -0.5 < v_1(0)+v_2(0) < 0.5 \end{cases} \tag{17}$$

where $u(0)$ is the initial battery current value when the following data is utilized to identify the parameters. The constraints of $v_1(0)$, $v_2(0)$ and $v_1(0)+v_2(0)$ are obtained from the battery voltage when charging or discharging the battery with the maximum allowable current. Because E_o ranges from 3.5 to 4.05 V and the battery terminal voltage v_o ranges from 4.05 V to 3 V when the battery is charged or discharged, the absolute value of maximum difference between E_o and v_o is less than 0.5 V. From Eq. (2), we can get $v_1(0)+v_2(0)$ are limited within $[-0.5, 0.5]$, therefore $v_1(0)$ and $v_2(0)$ are also with the same range. The initial values of $v_1(0)$, $v_2(0)$ and E_o are chosen randomly with the restriction in Eq. (17).

5.1. Battery parameter identification

Two hundred and fifty-three cycles are applied on the energy decay experiment, partial experiment data is shown in Fig. 4.

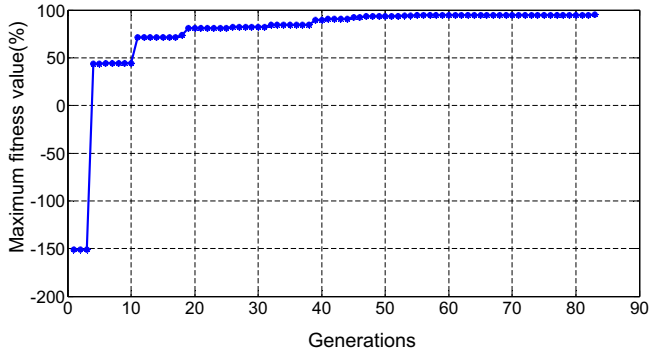

Fig. 8. Maximum fitness value in each generation of GA.

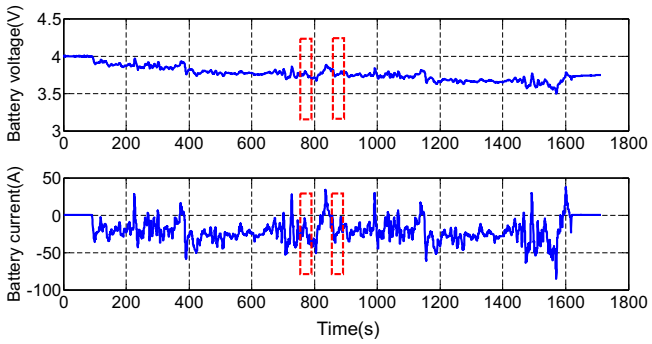

Fig. 9. Battery current and voltage.

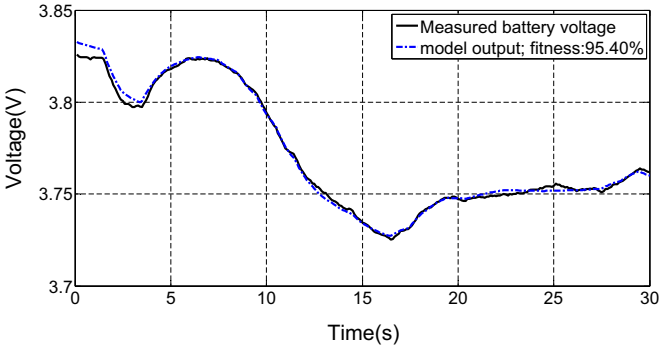

Fig. 11. Comparison of measured battery voltage and model output for time period of 850 s–880 s.

Among them, we conducted the experiment with the following pattern: at C/2 (16 A) charge rate and 1 C (32 A) discharge rate, 2 C charge rate and 2 C discharge rate, 1 C charge rate and 2 C discharge rate, 1 C charge rate and at 1 C discharge rate for 109 cycles, 98 cycles, 43 cycles and 3 cycles, respectively. The initial capacity is 32 Ah. After 253 cycles, the battery capacity drops to less than 23 Ah. There is 1 min rest for the battery after charging for 12 min. Fig. 5 presents the measured battery terminal voltage of cycle 102. Three different testing periods marked on the curve are selected for the parameter identification. After the parameters are identified based on GA and PEM method, one of the identified results are shown in Fig. 6, in which the fitness can reach 95.28% which satisfies the criteria presented in Section 3. Fig. 7 presents the differences between measured voltage and model output, of which the maximum error is less than 0.006 V. This indicates that the model can simulate the battery voltage with good accuracy.

Fig. 8 shows the maximum fitness value in each iteration generation of GA, which is calculated using Eq. (9). The initial maximum fitness value is −150.86%, and after 83 generations, the maximum fitness value reaches 95% and GA calculation terminates. The whole process lasts 5 min using a laptop with a CPU core i5 and 4G RAM.

Fig. 9 shows the measured terminal voltage and current curves of a used battery when the battery is simulated with a hardware-in-the-loop system with an urban dynamometer driving schedule (UDDS) drive cycle. Similar to Fig. 5, the data marked within red rectangle frames is extracted to estimate the system parameters. The results are shown in Figs. 10 and 11 respectively.

It can be seen from Figs. 10 and 11 that the identified terminal voltage can track the measured terminal voltage of the battery, and the fitness function can reach 95.12% and 95.40%, respectively. Fig. 12 shows the minimum V_n variation of each generation during evolution process for time period 850 s–880 s. The beginning value is 6.620 V^2 and it gradually converges during evolution. After 46 generations, it reduces to less than 0.005 V^2 when the GA calculation terminates. The whole calculation lasts less than 5 min. It is therefore proves that the proposed GA can estimate the battery parameters even when the vehicle is in operation. Based on the identified results of different cycle data, partial data are listed in Table 1, which includes R_{diff}, C_{diff}, battery capacity, battery average temperature and measured battery SOH inferred from battery diffusion capacitance.

In Table 1, R_{diff} and C_{diff} are the online identified diffusion resistance and capacitance value. The capacity denotes the battery discharge capacity at 1 C current rate after the battery is fully charged. The temperature is the average battery temperature when identifying the parameters. It can be seen from Table 1 that the diffusion resistance R_{diff} remains almost unchanged but the diffusion capacitance C_{diff} decreases gradually as the battery ages. The capacitance varies from 1629.04 F to 459.42 F as the battery capacity varies from 31.37 Ah to 22.77 Ah. Hence the change of diffusion capacitance can reflect the change of battery capacity, i.e., battery SOH. Based on the identified C_{diff} and the related capacity of each measurement, a linear equation with the reciprocal of C_{diff}, as shown in Eq. (18), can be obtained to calculate the battery SOH h at room temperature.

$$h = \left(\frac{b_1 \cdot C_{diff\_rat}}{C_{diff}} + b_0\right) \times 100\% \tag{18}$$

where $b_0 = 1.105$, $b_1 = -0.105$, C_{diff_rat} is the identified capacitance for a healthy battery and equals 1632.36 F. In Table 1, the battery SOH calculated using C_{diff} and capacity measurement, as well as their difference are presented. The maximum error is 4.35%.

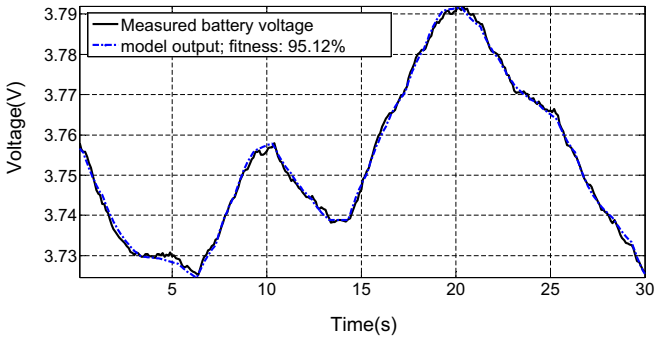

Fig. 10. Comparison of measured battery voltage and model output for time period of 750 s–780 s.

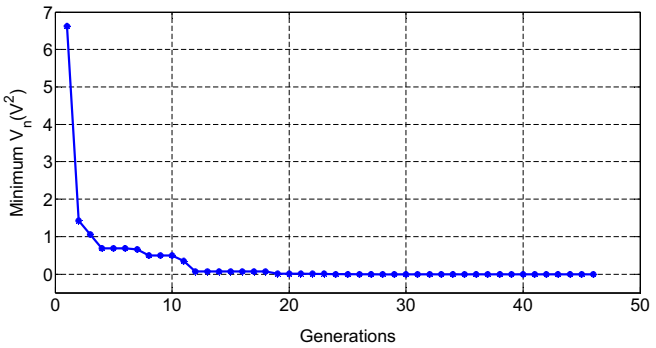

Fig. 12. Minimum V_n variation during evolution process for time period 850 s–880 s.

Table 1
The identified battery parameters.

Cycle no.	R_{diff} (Ω)	C_{diff} (F)	Capacity (Ah)	Temperature (°C)	SOH calculated using C_{diff} (%)	SOH calculated using capacity (%)	SOH error (%)
14	0.0024	1629.04	31.37	23.03	99.98	98.03	1.95
50	0.0020	1502.96	30.98	22.02	99.10	96.82	2.27
102	0.0019	1527.56	30.38	21.55	99.28	94.93	4.35
126	0.0021	1202.41	29.95	22.36	96.25	93.59	2.65
158	0.0020	855.30	28.15	21.75	90.46	87.97	2.49
172	0.0019	765.86	27.87	23.08	88.12	87.09	1.03
188	0.0020	606.70	27.11	25.32	82.25	84.72	−2.47
208	0.0022	578.25	26.19	24.58	80.86	81.84	−0.98
231	0.0025	502.90	24.39	25.18	76.42	76.22	0.20
253	0.0027	459.42	22.77	25.78	73.19	71.16	2.04

5.2. Temperature influence

The battery parameters and capacity change with temperature. In order to ensure the robustness of the proposed method, temperature influence is taken into account to increase the identification accuracy and robustness. A healthy battery is experimented in a temperature-controlled chamber. A standard battery test equipment BT 2000, a product of Arbin Instruments Inc., is used to test the battery performance with C/2 charge rate and 1 C discharge rate. In an electric drive vehicle, the battery pack is equipped with an effective thermal control module, which usually can maintain the battery temperature within 0 °C–40 °C. Therefore, we test the battery at different ambient temperatures from 0 °C to 40 °C with 5 °C increment as a next step. Table 2 presents the battery capacity versus different temperatures. The parameters of the battery at different temperatures are identified as well and shown in Table 2. From Table 2, C_{diff} changes from 504.47 F at 0 °C to 2172.28 F at 40 °C; and R_{diff} changes from 0.0056 Ω at 0 °C to 0.0016 Ω at 40 °C. The battery capacity will increase from 26.47 Ah at 0 °C to 33.84 Ah at 40 °C.

Fig. 13 presents the resistance and capacitance variation at different temperatures. No doubt, the resistance decreases and the capacitance increases as the temperature increases, thus it can reflect the battery capacity variation, as shown in Fig. 14.

Table 2
The identified battery parameters with different temperatures.

Temperature (°C)	R_{diff} (Ω)	C_{diff} (F)	Capacity (Ah)
0	0.0056	504.47	26.47
5	0.0033	821.23	28.64
10	0.0030	927.11	29.78
15	0.0026	1157.61	31.48
25	0.0022	1632.36	32.47
30	0.0020	1661.91	33.19
35	0.0018	1864.56	33.35
40	0.0016	2172.28	33.84

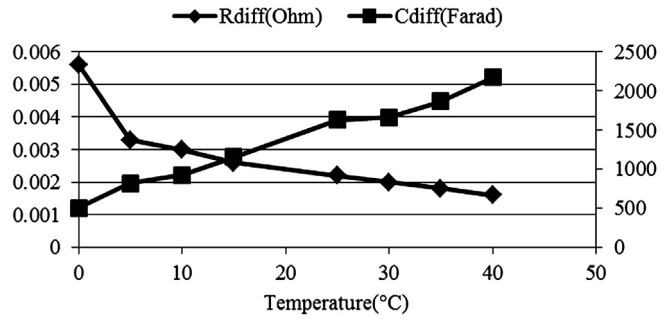

Fig. 13. Resistance and capacitance variation with temperature.

5.3. SOH estimation

Based on the analysis, Eq. (18) and the data listed in Table 2, the battery SOH h, as defined in Eq. (1), can be determined by the diffusion capacitance C_{diff} and temperature T through curve fitting.

$$h = f\left(C_{diff}, T\right) = \left(\frac{(a_1T^2 + a_2T + a_3)\cdot C_{diff\_rat}}{1000 \times C_{diff}} + b_0\right) \times 100\% \quad (19)$$

where $b_0 = 1.105$, $a_1 = 0.0041$, $a_2 = -2.684$, $a_3 = -35.12$, C_{diff_rat} is the identified capacitance for a healthy battery at 25 °C and equals 1632.36 F.

In order to verify the proposed algorithm, a used battery is tested at 5 °C and room temperature consecutively. The measured current and terminal voltage of the battery at 5 °C are shown in Fig. 15. The battery charging current is 16 A and discharging current is 32 A. The fully charged voltage is 4.05 V and the cut-off voltage for discharge is 3 V.

Based on the proposed method, the identified model output is compared to the measure battery terminal voltage as shown in Fig. 16. The fitness value reaches 95.35%, which satisfies the criteria

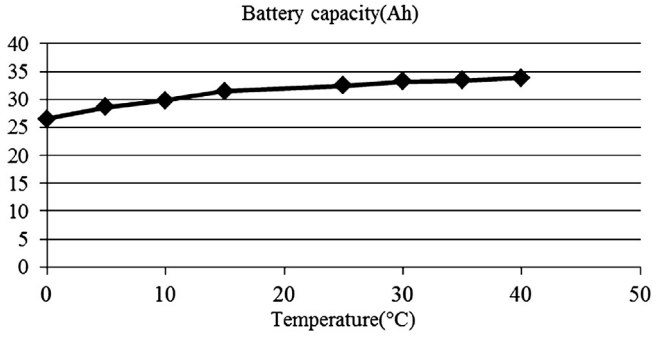

Fig. 14. Battery capacity variation with temperature.

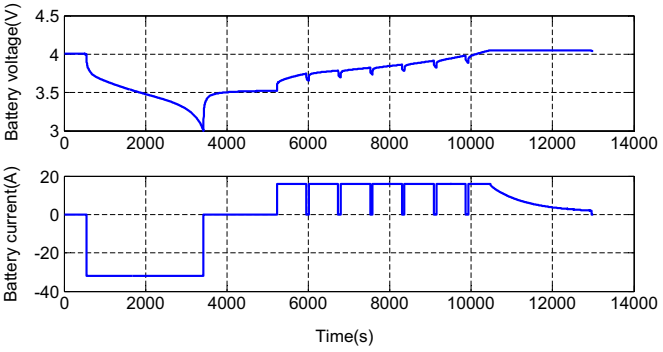

Fig. 15. The measured battery current and terminal voltage at 5 °C.

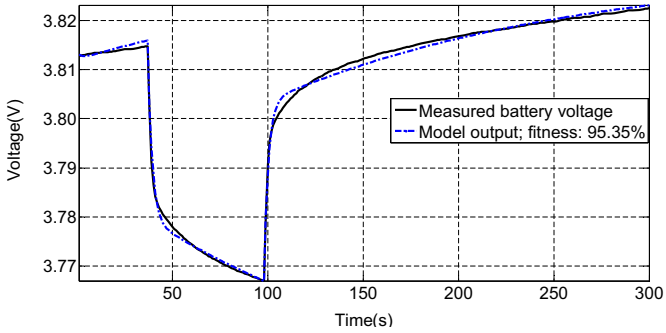

Fig. 16. Comparison of measured battery terminal voltage and the identified result.

of estimation precision. The difference between identified and measured battery voltage is within 0.006 V. The diffusion capacitance C_{diff} is 641.33 F. Substitute the value of C_{diff} and battery temperature into Eq. (19), the SOH is obtained, which is 98.14%. Through the following experiment at room temperature, the measured battery capacity at room temperature is 29.77 Ah, i.e., the battery SOH is 93.03%. The SOH difference is 5.11%. Thus it verifies the feasibility of the proposed method with different temperatures.

6. Conclusion

In this paper, battery SOH is estimated online by using the diffusion capacitance of a two-order RC circuit model of the lithium-ion battery. Genetic algorithm is proposed to estimate the parameters of the battery. The following conclusions can be made from the simulation and experiment results of the research.

- At the same temperature, battery SOH can be observed through C_{diff}. If C_{diff} drops, the battery capacity drops proportionally with the reciprocal of C_{diff}. SOH is proportional to the reciprocal of diffusion capacitance of the battery.
- Battery diffusion capacitance can be observed online and real time using genetic algorithm using measurement of battery current and terminal voltage.
- The battery capacity increases as the temperature rises. When the battery temperature increases, C_{diff} will increase and R_{diff} will decrease accordingly.

However, the GA needs some time to find the optimal values. We plan to improve the convergence speed of the GA in our future research.

References

[1] M. Coleman, L. Chi Kwan, Z. Chunbo, W.G. Hurley, Industrial Electronics, IEEE Transactions 54 (2007) 2550–2557.
[2] H. He, X. Zhang, R. Xiong, Y. Xu, H. Guo, Energy 39 (2012) 310–318.
[3] H. Hongwen, X. Rui, Z. Xiaowei, S. Fengchun, F. JinXin, Vehicular Technology, IEEE Transactions 60 (2011) 1461–1469.
[4] C. Hu, B.D. Youn, J. Chung, Applied Energy 92 (2012) 694–704.
[5] K. Jonghoon, B.H. Cho, Vehicular Technology, IEEE Transactions 60 (2011) 4249–4260.
[6] H. Tingshu, B. Zanchi, Z. Jianping, Energy Conversion, IEEE Transactions 26 (2011) 787–798.
[7] K.S. Ng, C.-S. Moo, Y.-P. Chen, Y.-C. Hsieh, Applied Energy 86 (2009) 1506–1511.
[8] M. Coleman, W.G. Hurley, L. Chin Kwan, Energy Conversion, IEEE Transactions 23 (2008) 708–713.
[9] K. Goebel, B. Saha, A. Saxena, J. Celaya, J. Christophersen, Instrumentation and Measurement Magazine, IEEE 11 (2008) 33–40.
[10] B. Saha, K. Goebel, S. Poll, J. Christophersen, Instrumentation and Measurement, IEEE Transactions 58 (2009) 291–296.
[11] J. Remmlinger, M. Buchholz, M. Meiler, P. Bernreuter, K. Dietmayer, Journal of Power Sources 196 (2011) 5357–5363.
[12] K. Jonghoon, L. Seongjun, B.H. Cho, Power Electronics, IEEE Transactions 27 (2012) 436–451.
[13] I.L.-S. Kim, Power Electronics, IEEE Transactions 25 (2010) 1013–1022.
[14] B.S. Bhangu, P. Bentley, D.A. Stone, C.M. Bingham, Vehicular Technology, IEEE Transactions 54 (2005) 783–794.
[15] C.R. Gould, C.M. Bingham, D.A. Stone, P. Bentley, Vehicular Technology, IEEE Transactions 58 (2009) 3905–3916.
[16] B. Pattipati, C. Sankavaram, K. Pattipati, Systems, Man, and Cybernetics, Part C: Applications and Reviews, IEEE Transactions 41 (2011) 869–884.
[17] Y. Zhang, C.-Y. Wang, X. Tang, Journal of Power Sources 196 (2011) 1513–1520.
[18] H. Bai, Y. Zhang, C. Semanson, C. Luo, C.C. Mi, Electrical Systems in Transportation, IET 1 (2011) 3–10.
[19] G. Crevecoeur, P. Sergeant, X.L. Dupre, R. Van de Walle, Magnetics, IEEE Transactions 46 (2010) 2585–2595.
[20] G. Rudolph, Neural Networks, IEEE Transactions 5 (1994) 96–101.
[21] L. Yee, G. Yong, X. Zong-Ben, Neural Networks, IEEE Transactions 8 (1997) 1165–1176.
[22] W. Lianghong, W. Yaonan, Y. Xiaofang, C. Zhenlong, Vehicular Technology, IEEE Transactions 60 (2011) 2458–2470.
[23] Y. He, W. Liu, B.J. Koch, Journal of Power Sources 195 (2010) 2969–2974.
[24] Y. Hu, S. Yurkovich, Journal of Power Sources 196 (2011) 2913–2923.
[25] Y. Hu, S. Yurkovich, Y. Guezennec, B.J. Yurkovich, Control Engineering Practice 17 (2009) 1190–1201.
[26] T. Söderström, P. Stoica, System Identification, Prentice Hall, 1989.
[27] Y. Jiang, K. Tu, Z. Hao, R. Cai, "The analysis and improvement of computational efficiency for a pseudo genetic algorithm," in: 2009 International Conference on Test and Measurement, ICTM 2009, December 5, 2009–December 6, 2009, Hong Kong, Hong Kong, 2009, pp. 413–417.